

# UCSF

## UC San Francisco Previously Published Works

### Title

Endovascular Ion Exchange Chemofiltration Device Reduces Off-Target Doxorubicin Exposure in a Hepatic Intra-arterial Chemotherapy Model

### Permalink

<https://escholarship.org/uc/item/3pc2z7sd>

### Journal

Radiology Imaging Cancer, 1(1)

### ISSN

2638-616X

### Authors

Yee, Colin  
McCoy, David  
Yu, Jay  
[et al.](#)

### Publication Date

2019-09-01

### DOI

10.1148/rycan.2019190009

Peer reviewed

# Endovascular Ion Exchange Chemofiltration Device Reduces Off-Target Doxorubicin Exposure in a Hepatic Intra-arterial Chemotherapy Model

Colin Yee, BS • David McCoy, MSc • Jay Yu, MS • Aaron Losey, MD • Caroline Jordan, PhD • Terilyn Moore, BSRT • Carol Stillson, RVT • Hee Jeung Oh • Bridget Kilbride • Shuvo Roy, PhD • Anand Patel, MD • Mark W. Wilson, MD • Steven W. Hetts, MD • on behalf of the ChemoFilter Consortium\*

From the Department of Radiology and Biomedical Imaging (C.Y., D.M., J.Y., A.L., C.L., T.M., C.S., B.K., A.P., M.W.W., S.W.H.) and Department of Bioengineering and Therapeutic Sciences (S.R.), University of California, San Francisco, 505 Parnassus Ave, L-351, San Francisco, CA 94143-0628; and Department of Chemical and Biomolecular Engineering, University of California, Berkeley, Berkeley, Calif (H.J.O.). Received April 8, 2019; revision requested April 18; revision received July 5; accepted July 25. Address correspondence to S.W.H. (e-mail: [steven.hetts@ucsf.edu](mailto:steven.hetts@ucsf.edu)).

Supported by the National Cancer Institute (R01CA194533).

\*For members of the ChemoFilter Consortium, please see the Acknowledgments.

Conflicts of interest are listed at the end of this article.

Radiology: Imaging Cancer 2019; 1(1):e190009 • <https://doi.org/10.1148/rycan.2019190009> • Content codes: **RO** **GI**

**Purpose:** To determine if endovascular chemofiltration with an ionic device (ChemoFilter [CF]) can be used to reduce systemic exposure and off-target biodistribution of doxorubicin (DOX) during hepatic intra-arterial chemotherapy (IAC) in a preclinical model.

**Materials and Methods:** Hepatic IAC infusions were performed in six pigs with normal livers. Animals underwent two 10-minute intra-arterial infusions of DOX (200 mg) into the common hepatic artery. Both the treatment group and the control group received initial IAC at 0 minutes and a second dose at 200 minutes. Prior to the second dose, CF devices were deployed in and adjacent to the hepatic venous outflow tract of treatment animals. Systemic exposure to DOX was monitored via blood samples taken during IAC procedures. After euthanasia, organ tissue DOX concentrations were analyzed. Alterations in systemic DOX exposure and biodistribution were compared by using one-tailed *t* tests.

**Results:** CF devices were well tolerated, and no hemodynamic, thrombotic, or immunologic complications were observed. Animals treated with a CF device had a significant reduction in systemic exposure when compared with systemic exposure in the control group ( $P < .009$ ). Treatment with a CF device caused a significant decrease in peak DOX concentration (31%,  $P < .01$ ) and increased the time to maximum concentration ( $P < .03$ ). Tissue analysis was used to confirm significant reduction in DOX accumulation in the heart and kidneys ( $P < .001$  and  $P < .022$ , respectively). Mean tissue concentrations in the heart, kidneys, and liver of animals treated with CF compared with those in control animals were  $14.2 \mu\text{g/g} \pm 1.9$  (standard deviation) versus  $26.0 \mu\text{g/g} \pm 1.8$ ,  $46.4 \mu\text{g/g} \pm 4.6$  versus  $172.6 \mu\text{g/g} \pm 40.2$ , and  $217.0 \mu\text{g/g} \pm 5.1$  versus  $236.8 \mu\text{g/g} \pm 9.0$ , respectively. Fluorescence imaging was used to confirm in vivo DOX binding to CF devices.

**Conclusion:** Reduced systemic exposure and heart bioaccumulation of DOX during local-regional chemotherapy to the liver can be achieved through in situ adsorption by minimally invasive image-guided CF devices.

© RSNA, 2019

Hepatocellular carcinoma (HCC) accounts for 80%–90% of primary liver cancer cases and is the fourth most common cause of cancer death, claiming 745 533 lives globally in 2012 (1). Patients with early-stage HCC can undergo curative surgical resection or liver transplantation (2,3). Unfortunately, 70%–80% of patients do not qualify for surgery because of advanced HCC progression. For patients with unresectable tumors, the current standard of care includes transarterial chemoembolization (TACE), drug-eluting bead TACE, and hepatic intra-arterial chemotherapy (IAC) to limit tumor growth (4,5). These image-guided local-regional therapies exploit dose-dependent antitumor effects of chemotherapeutic agents by selective administration to the arteries feeding the tumor (6–8). Although selective delivery has shown improved treatment outcomes and lower toxicities, these therapies have not improved survival for most patients with advanced HCC (2,9).

Interventional radiology techniques have been developed to improve the local delivery of chemotherapeutic drugs while diminishing systemic toxicity. Percutaneous hepatic perfusion (PHP) with simultaneous hemofiltration is a technique that relies on isolation of the hepatic venous outflow between occlusive endovenous balloons in the inferior vena cava (IVC) and an extracorporeal activated carbon hemofiltration circuit to remove the chemotherapeutic drug (10–12). Although highly efficient venous drug removal can be achieved (13), the system is hemodynamically disruptive and lacks adsorption specificity, removing essential blood components, including proteins, catecholamines, and cells (14,15).

Doxorubicin (DOX) is an effective chemotherapeutic agent for many tumors, but it is dose-limited due to irreversible cardiomyopathy caused by chronic or repeated systemic exposure. DOX administration at doses low enough to minimize cardiac toxicity also reduces its antitumor

## Abbreviations

AUC = area under curve, CF = ChemoFilter, DOX = doxorubicin, HCC = hepatocellular carcinoma, IAC = intraarterial chemotherapy, IVC = inferior vena cava, PHP = percutaneous hepatic perfusion, SAC-IER = strong acid cation ion exchange resin, TACE = transarterial chemoembolization

## Summary

Image-guided endovascular chemofiltration with ionic endovascular devices placed nonocclusively in the hepatic venous outflow tract and inferior vena cava during hepatic artery doxorubicin infusion reduced off-target blood and tissue concentrations of doxorubicin in a translational model.

## Key Points

- Adsorption of doxorubicin to an endovascular device placed temporarily in the hepatic venous outflow tract during hepatic artery chemotherapy reduces systemic concentrations of doxorubicin, thus reducing the potential for systemic toxic side effects at a particular drug dose or permitting dose escalation for better tumor control with a similar toxic side-effect profile.
- In situ drug adsorption in the veins draining an organ targeted with intraarterial chemotherapy enables drug binding without the marked hemodynamic effects associated with extracorporeal filtration systems.

effect (16,17). Strong acid cation ion exchange resins (SAC-IER) can selectively adsorb charged molecules such as DOX (18). Patel et al (19) previously constructed ChemoFilter (CF) devices from SAC-IER membranes that reduced the peak blood concentrations of DOX by 85% during infusion of the drug in the IVC just below the device in the infrarenal IVC in a preclinical porcine model. Those membranous CF devices, however, were mechanically unstable, prompting development of more durable CF devices containing drug-binding SAC-IER beads within nylon pouches.

There is a clinical need for a CF device that is deployable and minimally invasive and that could selectively filter drugs in situ at high extraction efficiencies. In this study, we evaluated the ability of endovascular chemofiltration using an ionic device to reduce systemic exposure and off-target biodistribution of DOX during hepatic IAC in a preclinical model.

## Materials and Methods

Our study was divided into two phases: Phase 1 was in vitro characterization of the ability of CF prototypes to selectively bind DOX. Phase 2 was in vivo evaluation of the ability of CF devices to decrease systemic exposure and alter biodistribution of DOX during high-dose IAC.

### Phase 1: In Vitro Characterization of CF Drug Binding

CF prototypes were designed with a tapered cylindrical shape (Fig 1b, 1c) to allow deployment of multiple devices through a single-access sheath while maximizing the amount of drug-binding material. Each CF device contained  $1.20 \text{ g} \pm 0.5$  (mean  $\pm$  standard deviation) of SAC-IER (Dowex; Dow Chemical Company, Midland, Mich), an amount previously optimized experimentally in vitro. The drug-binding material was contained in a  $0.5 \times 23$  cm porous nylon mesh cylinder (NITEX 03-250/50;

SEFAR, Thai, Switzerland) with 250- $\mu\text{m}$  pores to promote adequate diffusion of the drug to the filtration material under blood flow. Device design was predicated on prior experiments varying pore size, physical dimensions, and chemistries (18–20). To assess drug binding, CF prototypes were tested in a flow circuit mimicking physiologic conditions (19,20). The flow circuit consisted of 0.25-inch tubing (L/S 24; Masterflex, Gelsenkirchen, Germany) connected to a 1-L reservoir. Flow was maintained at a human hepatic vein blood flow rate (750 mL/min) with a peristaltic pump (L/S; Masterflex). Porcine blood solutions with 50 mg (0.05 mg/mL) of DOX, maintained at 37°C, were used to simulate a standard clinical dose used in TACE and IAC procedures. Time points were taken from 0 to 60 minutes to measure the clearance rates and adsorption capacity of CF prototypes.

### Phase 2: In Vivo Evaluation of Intravascular Chemofiltration

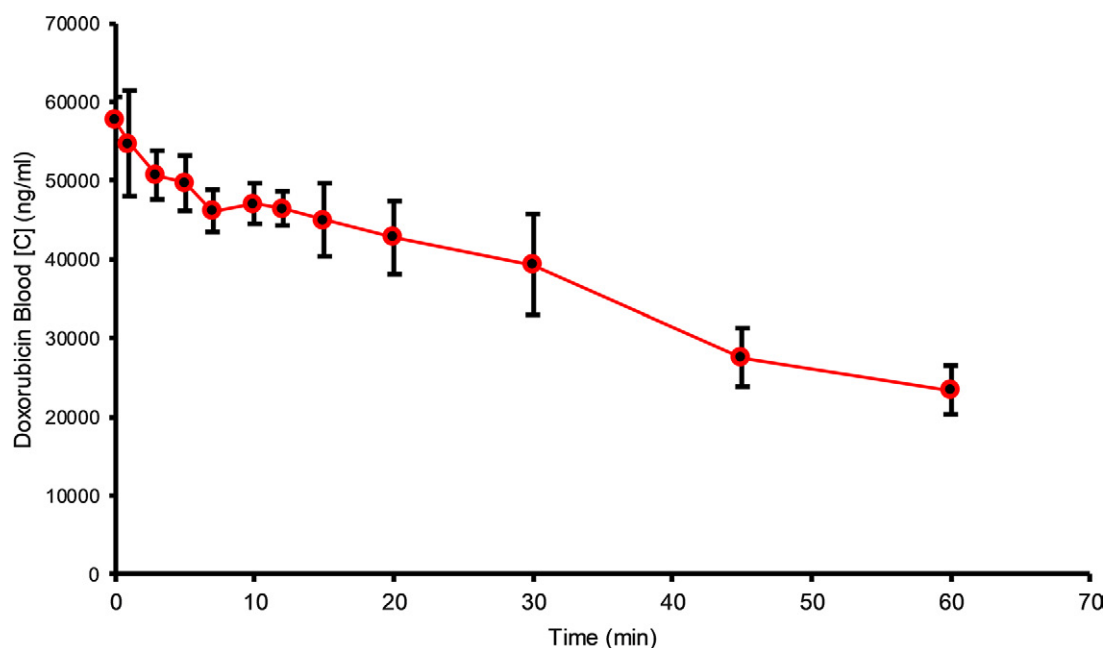
To provide trackability during deployment and retrieval in vivo, CF devices developed in phase 1 were mounted on 0.038-inch hydrophilic guide wires (Glidewire; Terumo, Tokyo, Japan) using medical-grade polyester shrink wrap (Advanced Polymers, Salem, NH). Tungsten radiopaque marker bands were added to the proximal and distal tips of the CF to aid in image-guided placement during x-ray fluoroscopic procedures.

**Study design.**—Experimental approval was obtained from the institutional committee on animal research. A multidose hepatic IAC porcine model was used to evaluate the ability of intravascular chemofiltration to reduce systemic exposure and bioaccumulation in vivo. The experimental design is shown in Figure 2.

Previous animal experiments ( $n = 12$ ) were conducted to study the drug capture capabilities and pharmacokinetic alterations of CF prototypes during hepatic IAC. However, upon review of the results, the pharmacokinetic parameters were shown to be highly variable after IAC with DOX between control animals and animals treated with CF. We concluded the inconsistent pharmacokinetic data were due to the variability in DOX metabolism seen in young pig livers during IAC. To overcome the variability in drug metabolism, we implemented a multidose IAC study design similar to the method previously developed to study the performance of advanced drug delivery systems (21,22). The multidose IAC consists of two treatments in which the initial IAC is used as a reference phase allowing each animal to serve as its own control, while the second dose is used to examine the effects of CF treatment during IAC.

Animals were divided into two experimental groups: Those in group 1 (IAC only [control group],  $n = 3$ ) were treated with two hepatic IAC infusions at 0 and 120 minutes without CF devices. Those in group 2 (IAC with CF [treatment group],  $n = 3$ ) were treated with one hepatic IAC infusion without the device (intrasubject physiologic control) and then a second IAC infusion with the CF device in place.

**Experimental procedure.**—Experiments were performed according to the *Guide for the Care and Use of Laboratory Animals*. Six female Yorkshire pigs (mean weight, 42 kg  $\pm$  6) (Pork Power Farms, Turlock, Calif) with normal livers were used.



a.



b.



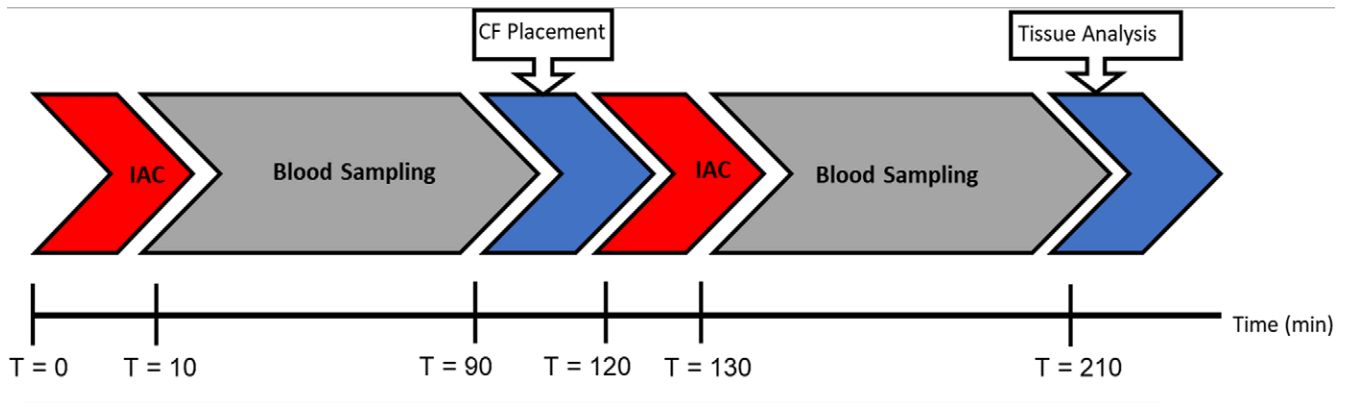
c.

**Figure 1:** In vitro flow model experiments. **(a)** Graph shows doxorubicin (DOX) filtration over the course of 60 minutes from porcine whole blood (0.05 mg/mL DOX) ( $n = 6$ ). Data are presented as mean  $\pm$  standard deviation. **(b, c)** Photographs of the Chemofilter device before **(b)** and after **(c)** the flow model experiment.

Interventions were performed by practicing neurointerventional (S.W.H., >15 years of experience) and interventional (M.W.W., >20 years of experience) radiologists. Pigs were acclimatized for 48 hours and fasted for 8–18 hours before experiments. Animals were anesthetized by using acepromazine and ketamine and were maintained with isoflurane. Blood pressure and oxygen saturation levels were continuously monitored during the procedure. Two 6-F vascular sheaths were placed in the left common femoral vein and right common femoral artery; the right internal jugular vein was accessed with US guidance via sequential dilation to allow placement of an 18-F vascular sheath. Animals were administered heparin (70 U per kilogram of body weight) intravenously. The arterial sheath was used to access the hepatic artery for IAC injections using a 5-F Cobra catheter (Glidecath; Terumo). Prior to IAC, the gastroduodenal artery was embolized to prevent reflux of DOX toward the gastrointestinal tract. Depending on the animal's

vascular anatomy, gastroduodenal artery embolization was performed by using three to five embolic coils (TRUFILL; Cordis, Fremont, Calif). The gastroduodenal artery in one animal from group 1 was not embolized due to its small size. Angiograms were obtained via injection of contrast material (Omnipaque 300; GE Healthcare, Waukesha, Wis) (Fig 3). CF devices were deployed with fluoroscopic guidance (S.W.H., M.W.W) through the 18-F sheath and were positioned in the hepatic veins and IVC adjacent to the hepatic venous confluence (Fig 3).

The original prospective study design anticipated devices being deployed in each hepatic vein to capture the infused drug directly at venous outflow before dilution into the IVC. However, due to the complex vasculature and rigidity of the devices, access to more than one hepatic vein was not feasible. Attempts were made to navigate all CF devices into the hepatic veins, as devices in the hepatic veins would be expected to be



Group	Treatment #1, 0-90 min	Treatment #2, 120-210 min
Group 1	IAC Doxorubicin, 2.0 mg/ml, 100 ml	IAC Doxorubicin, 2.0 mg/ml, 100 ml
Group 2	IAC Doxorubicin, 2.0 mg/ml, 100 ml	IAC+CF Doxorubicin, 2.0 mg/ml, 100 ml

**Figure 2:** Experimental protocol for blood and tissue sampling in vivo. The animals in each experimental group underwent a 10-minute intra-arterial infusion of doxorubicin (DOX) (2 mg/mL, 100 mL) at 0 and 120 minutes. Prior to administration of the second dose of DOX in group 2, ChemoFilter (CF) devices were deployed. Blood samples were collected at various timepoints during each treatment for pharmacokinetic analysis. After treatment, the pigs were euthanized and tissue analysis was performed. IAC = intraarterial chemotherapy.

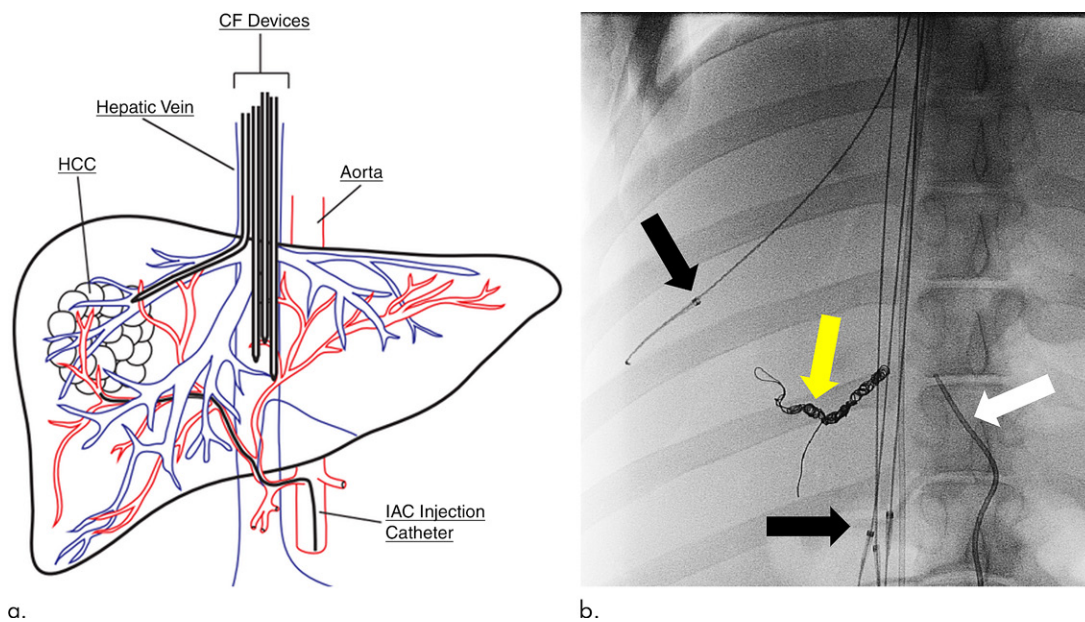


**Figure 3:** ChemoFilter (CF) device deployment in vivo. **(a)** Schematic drawing of CF devices in place during local-regional treatment of the liver during intra-arterial chemotherapy (IAC). As doxorubicin (DOX) is being infused into the hepatic artery, the CF devices are placed in the venous outflow of the liver. **(b)** Fluoroscopic image of the in vivo experiments showing deployed CF devices placed in the hepatic vein and inferior vena cava during IAC. Black arrows = distal markerband of CF, white arrow = IAC infusion catheter. Note that gastroduodenal artery has been embolized with coils (yellow arrow) to prevent redirection of DOX away from the liver during IAC.

exposed to a higher local concentration of DOX and thus have a better opportunity to adsorb the drug. However, because of the angles of some hepatic veins and the stiffness of the CF devices, a fallback position of placing CF devices in the IVC at and just above the hepatic venous confluence was pursued so as to deploy as much absorptive surface area as possible between the liver (infused organ) and heart (site of primary toxicity).

Each animal underwent two separate high-dose IAC infusions of DOX at 0 and 120 minutes (ie, each animal served as its own control given potential differences in metabolism between individuals). The initial IAC treatment at 0 minutes was used as a reference phase, and the second dose at 120 minutes was used as the treatment phase. Each individual IAC procedure lasted 90 minutes to mimic clinical TACE procedures. A total



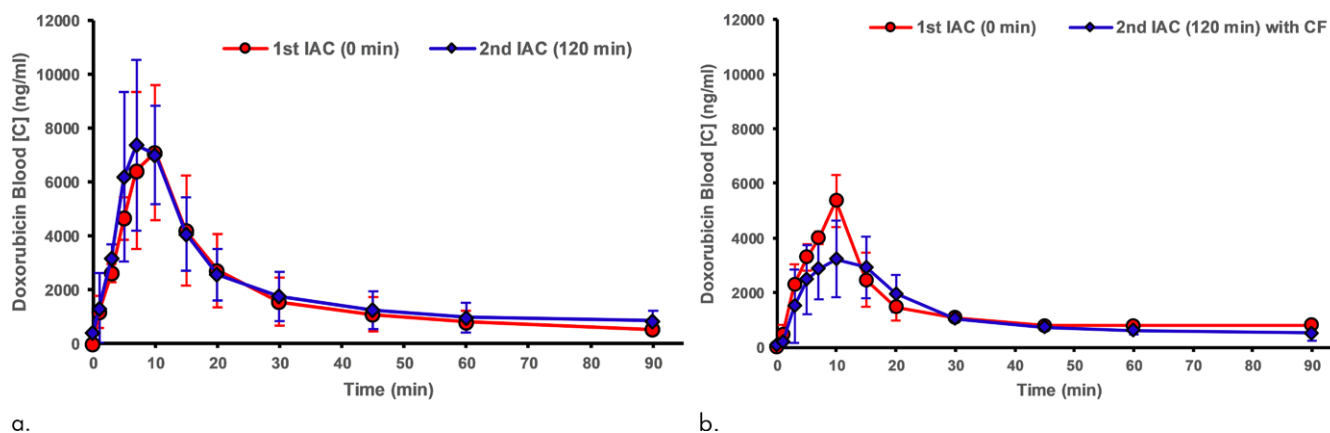


**Figure 4:** Blood concentration–time profiles of doxorubicin during in vivo experiments. ChemoFilter (CF) devices decrease peak doxorubicin (DOX) concentration and reduce the area under the curve for drug exposure. The graphs compare profiles of DOX during the first (blue) and second (red) intra-arterial chemotherapy (IAC) infusions for **(a)** group 1 (IAC vs IAC,  $n = 3$ ) and **(b)** group 2 (IAC vs IAC and CF,  $n = 3$ ). Data are mean  $\pm$  standard deviation.

of 200 mg of Doxorubicin HCl (2 mg/mL, 100 mL total; Pfizer, New York, NY) was administered at a flow rate of 10 mL/min over 10 minutes by using a syringe pump (NE-4000; PumpSystems, Farmington, NY). Blood samples were drawn from the common femoral vein at 0, 1, 3, 5, 7, 10, 12, 15, 20, 30, 45, 60, and 90 minutes relative to the initiation of DOX infusion to monitor systemic DOX concentration.

All animals were euthanized per institutional protocol immediately after the 90-minute blood sample of the second IAC by injecting 100 mL of saturated KCl salt solution into the jugular access sheath. Tissues were harvested and stored at  $-20^{\circ}\text{C}$  until further analysis.

**DOX quantification.**—DOX concentrations in whole blood were determined by using a modified high-performance liquid chromatography method previously described (23). Separation was performed on a C18 reversed-phase column (Spherisorb ODS2; Waters, Milford, Mass) at a flow rate of 1 mL/min. The high-performance liquid chromatography machine (Agilent 1100 series; Agilent Technologies, Santa Clara, Calif) fluorescence detector was set at 480-nm excitation and 560-nm emission. DOX concentrations in the heart, liver, and kidneys were determined similarly. To measure DOX concentrations in tissue, organs were mixed with phosphate-buffered saline and homogenized until tissue concentrations reached 1 mg/mL. Tissue samples underwent the same extraction method as blood samples.

**CF drug binding.**—After treatment, the CF devices were retrieved before euthanasia and were washed twice in deionized water to remove blood on the surface. Fluorescence microscopy (Ti Microscope DS-Qi2; Nikon, Tokyo, Japan) with 485-nm excitation and 560-nm emission was used to verify the presence of DOX adsorbed by the device. Because of the self-quenching nature of DOX fluorescence at high concentrations, fluorescence microscopy was used to qualitatively measure the presence of adsorbed DOX.

### Statistical Analysis

Statistical analyses were conducted with software (R, version 3.5.1; R Foundation for Statistical Computing, Vienna, Aus-

tria). Area under the curve (AUC) was used to measure systemic exposure of DOX and was calculated by using natural cubic spline interpolation. DOX difference was calculated as concentration with the device minus concentration without it; therefore, the negative AUC of this difference over time represents the amount of absorption by the device. AUC with the device and AUC without it were calculated and plotted. Additionally, the concentration maximum ( $C_{\text{max}}$ ) and difference in concentration maximum ( $\Delta C_{\text{max}}$ ) were calculated for each infusion of DOX. The difference between measurements with the CF device versus those with no CF device was calculated for each measurement and compared between experimental groups. The tissue concentrations of DOX were calculated to compare drug uptake and accumulation between the experimental conditions. One-tailed  $t$  tests were used to compare DOX accumulation between experimental groups.

## Results

### Phase 1: In Vitro Characterization of CF Drug Binding

A flow circuit was used to evaluate the drug binding capacity and kinetics of CF prototypes under physiologic conditions. The DOX binding curves are displayed in Figure 1a. Single CF devices showed significant binding capacity, removing a mean of  $26 \text{ mg} \pm 3.5$  (51%,  $P < .05$ ) of DOX from blood in 60 minutes. The demonstrated capacity and binding kinetics observed within the flow model were used to further optimize the in vivo prototypes.

### Phase 2: In Vivo Evaluation of Intravascular Chemofiltration

CF devices were well tolerated in all treatment animals. No hemodynamic or thrombotic complications were observed. The original study design had devices deployed in each hepatic vein to capture the infused drug directly at the venous outflow before dilution in the IVC. However, due to the complex vasculature and rigidity of the devices, access to the hepatic vein was not feasible in one treatment animal in group 2. A total of 15 devices were used in treatment animals in group 2: four devices were deployed in two animals (one device in the right hepatic

**ChemoFilter Devices Decrease Systemic Exposure and Peak Doxorubicin Concentration**

Treatment (IAC vs IAC+CF)	$C_{Max}$ (ng/mL)	$\Delta C_{max}$	$\Delta C_{max}$ (%)	AUC Systemic (ng·min/mL)	$\Delta$ AUC Systemic (ng·min/mL)	$\Delta$ AUC Systemic (%)
<b>Group 1</b>						
IAC (0–90 min)	7930.3	370.8	5.0	168915.0	13990.7	8.2
IAC (120–210 min)	8301.0	...	...	182905.7	...	...
<b>Group 2</b>						
IAC (0–90 min)	4946.1	-1558.5	-31.5	112256.7	-22075.9	-19.7
IAC+CF (120–210 min)	3387.6	...	...	90180.8	...	...
<i>P</i> value	...	...	.014	...	...	<.01

Note.—Pharmacokinetic parameters of doxorubicin in vivo after multiple intraarterial chemotherapy (IAC) administrations. Data were from the systemic blood samples. AUC = area under the curve, CF = ChemoFilter,  $C_{max}$  = concentration maximum.  $\Delta C_{max}$  = change in  $C_{max}$  from second IAC minus first IAC.  $\Delta$ AUC systemic = [(AUCin2 - AUCin1)/AUCin1]  $\times$  100 (ie, change in AUC systemic from second IAC minus first IAC).

vein, three devices in the IVC), and seven devices were deployed in one animal (one device in the right hepatic vein, six devices in the IVC). Variations in the number of devices deployed were the result of changes in vascular anatomy from pig to pig and difficulties in deployment.

Pharmacokinetic analyses of IAC experiments are presented in Figure 4 and are summarized in the Table. Animals from group 2 (ie, those treated with CF devices) showed a significant reduction in peak DOX concentrations when compared with the first IAC infusions without CF devices in place (31.5%,  $P < .014$ ). Peak concentrations for group 1 (control animals) showed the opposite result, with higher peak concentrations during the second IAC infusions when compared with the reference infusion. Treatment with CF in the hepatic venous outflow tract reduced systemic exposure of DOX during IAC when compared with initial control infusions with no CF devices. Treatment with CF devices yielded a 19.7% decrease in systemic exposure (AUC) to DOX ( $P < .01$ ) as compared with control animals (Table).

**Tissue accumulation.**—Tissue concentrations of DOX in the heart and kidneys were measured to evaluate the reduction of DOX bioaccumulation in off-target organs from intravascular chemofiltration (Fig 5). Animals treated with CF devices showed a 46% reduction in DOX accumulation in the heart compared with control animals (mean, 14.2  $\mu$ g/g  $\pm$  1.9 vs 26.0  $\mu$ g/g  $\pm$  1.9;  $P < .001$ ). The greatest reduction in off-target exposure was detected in the kidneys, in which there was a 73% decrease in DOX accumulation (mean, 46.4  $\mu$ g/g  $\pm$  4.6 vs 172.7  $\mu$ g/g  $\pm$  40.2;  $P < .02$ ). The DOX concentration in the liver was measured to assess DOX delivery to the target organ. Liver concentrations of DOX also decreased 8.4% in animals treated with CF (mean, 236.9  $\mu$ g/g  $\pm$  9.0 vs 217.0  $\mu$ g/g  $\pm$  5.1;  $P < .035$ ).

**CF device drug binding.**—CF devices were viewed with a fluorescence microscope, and the fluorescence was used to detect bound DOX from in situ filtration (Fig 6c). The fluorescence of DOX on the CF device shows enhanced DOX binding on the

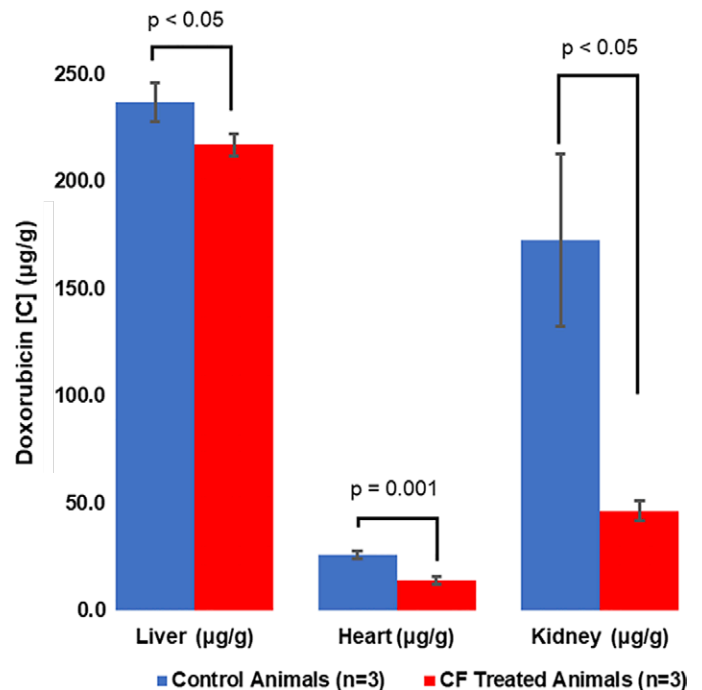


**Figure 5:** The ChemoFilter (CF) device reduces accumulation of doxorubicin (DOX) in off-target organs. Bar graph shows mean DOX concentrations in organs in groups 1 (IAC + IAC) and 2 (IAC + IAC with CF). Significant decreases in DOX accumulation were observed in all off-target organs (kidneys and heart) in animals treated with CF devices compared with control animals. Data are mean  $\pm$  standard deviation.

segments of CF devices placed near the hepatic venous confluence. This distribution of filtered DOX on CF devices suggests that removal of DOX can be enhanced by deploying CF devices directly adjacent to the venous drainage of the target organ.

## Discussion

Systemic toxicities limit the therapeutic efficacy of antineoplastic agents whether delivered systemically or local-regionally for aggressive diseases like HCC (24). Our study demonstrates that DOX can be selectively removed by intravascularly placed CF devices via ion exchange adsorption in situ from the he-

patric venous outflow during high-dose hepatic IAC. The design of this device allows large quantities of drug-binding material to be temporarily placed directly in the venous outflow of the liver. Multiple CF devices can be deployed simultaneously, increasing the adsorptive surface area. Furthermore, the device was not occlusive and allowed for adequate blood flow through the IVC while up to seven CF devices were deployed. In vivo pharmacokinetic and biodistribution analyses demonstrated significant reduction in systemic exposure ( $P < .01$ ) and off-target bioaccumulation of DOX within the heart and kidneys ( $P < .001$  and  $P < .02$ , respectively). This is an important step in the preclinical development of practical endovascular CF devices that could reduce off-target toxicity in patients undergoing chemotherapy.

TACE and drug-eluting bead TACE were developed to improve the efficacy of chemotherapy treatments by combining local and targeted drug delivery with concurrent embolization of the artery feeding the tumor (7,25). These treatments are based on the principle that increased exposure of cytostatic agents to the target tissues can be achieved by administering drugs directly to the feeding arteries of a tumor, thereby allowing higher exposure of chemotherapeutic agents by the tumor cells and creating a maximal therapeutic effect while minimizing the systemic drug exposure (26). However, systemic toxicities, low tissue concentrations, and lack of repeatability result in disease progression and development of multidrug resistance tumors (27,28). An additional argument for using intra-arterial DOX infusion without concomitant bead use is that DOX may not be as effective for HCC treatment in a hypoxic environment (29–31). Use of a CF could be valuable in combination with current intra-arterial therapies to mitigate systemic toxicities, as it could enable either similar tumor control with reduced off-target side effects at the same DOX infusion dose or dose escalation of DOX to achieve better tumor control.

Surgical therapies have shown promise in patients with advanced hepatic tumors by enabling use of chemotherapy above systemic maximum tolerated doses through vascular occlusion and extracorporeal hemofiltration (10,14,32). Isolated hepatic perfusion involves surgically isolating the vascular supply of the liver with subsequent hyperthermic perfusion of a high dose of chemotherapy into the hepatic artery (14,32,33). Isolated hepatic perfusion allows local treatment of tumors with sustained drug levels four to five times the maximum tolerated dose used during systemic administration (14) while avoiding potentially fatal toxicities. Tumor response rates are 37%–52% in patients with metastatic ocular melanoma (34) and 50%–60% in patients with liver metastases from colorectal carcinoma (35); there

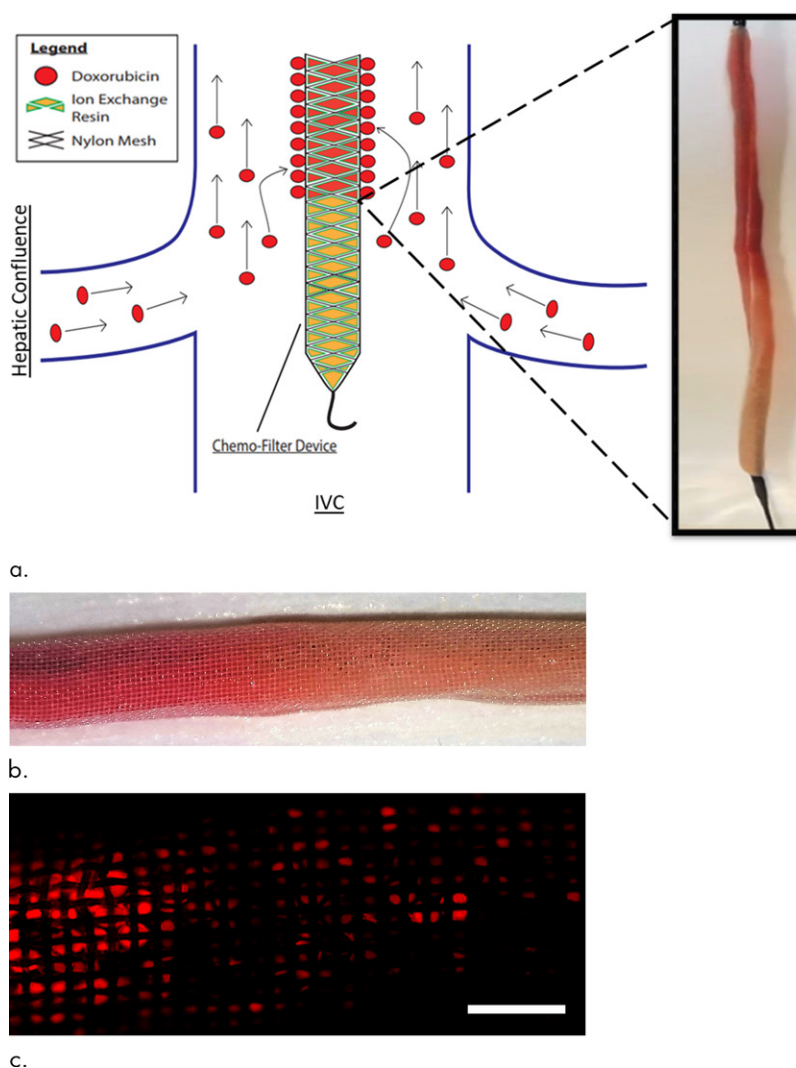


**Figure 6:** In situ doxorubicin (DOX) adsorption by the ChemoFilter (CF) device. **(a)** Schematic depicting in vivo DOX binding by CF device positioned adjacent to hepatic venous drainage. Prior to euthanasia, CF devices were retrieved through the jugular sheath and were washed with phosphate-buffered saline to remove adsorbed biomolecules. CF devices were viewed with a wide-field fluorescence microscope, and the fluorescence was used to detect DOX (red). Scale bars = 2 mm. **(b)** Distribution of filtered DOX (red) on CF devices relative to the hepatic venous outflow was observed (left side of image in **b** is equivalent to the cranial side in **a**). Enhanced DOX binding onto CF when positioned closer to the hepatic confluence. **(c)** Fluorescence microscopy was used to confirm DOX binding to strong acid cation ion exchange resin beads within the nylon sac. IVC = inferior vena cava.

is a remarkable 89% complete response rate in patients with unresectable sarcoma (36). Nevertheless, despite favorable response rates, the complexity and morbidity of the procedure and extensive postoperative care have limited clinical adoption of isolated hepatic perfusion.

PHP with simultaneous hemofiltration is a similar regional technique aimed at improving safety and local delivery and removing high-dose chemotherapeutic drugs from the tumor-bearing organ while reducing systemic toxicity. However, unlike the isolated hepatic perfusion circuit where chemotherapy drugs are extracted after perfusion, PHP relies on an extracorporeal activated carbon hemofiltration circuit to remove the drug (10–12), leading to delivery of higher concentrations of the drug during shorter treatment sessions. PHP is used to attain complete



endovascular isolation of the hepatic venous outflow via inflation of a double balloon catheter (Hepatic Chemosat; Delcath Systems, New York, NY) in the supra- and infrahepatic IVC and simultaneous pumping of blood from the isolated perihepatic IVC to an extracorporeal filter. PHP is effective in the treatment of melanoma liver metastases, with progression-free survival of 254 days when compared with 52 and 54 days for chemoembolization and yttrium 90 embolization, respectively (37), and increased hepatic progression-free survival (38). By using activated carbon as a filter material, PHP can remove a wide variety of cytotoxic agents, but unfortunately the lack of specificity also leads to removal of proteins, catecholamines, and cells (14,15). As a result of the nonspecific removal of blood components, patients frequently experience adverse effects, such as hypotension, thrombocytopenia, leukopenia, anemia, and neutropenia (35,37), which require plasma exchange, blood transfusions, and postoperative overnight intensive care. The lack of adsorption specificity, hemocompatibility, and the necessity for vascular isolation have limited the use of hemoperfusion techniques. Our study demonstrates selective filtration of the positively charged anthracycline DOX by negatively charged CF devices in situ, introducing the possibility of chemofiltration by a temporarily deployable endovascular device rather than an extracorporeal circuit.

There were several limitations to our study. Although the CF devices contained enough binding material to remove two times the administered DOX dose, the devices adsorbed, on average, 19.6% of the injected dose in vivo. The relatively low adsorption of DOX may relate to low hepatic venous blood concentrations due to rapid tissue uptake and elimination of the drug in vivo in the livers of healthy young pigs. To achieve enhanced drug removal, there is a need for optimized materials with increased selectivity and binding kinetics at low concentrations often seen in vivo. Recent studies (20,39) have demonstrated that incorporating DNA-based biomaterials into a CF device can result in increased drug removal when compared with SAC-IER devices. The tapered cylindrical shape of the CF device in this study allowed blood to flow around instead of through the binding material, limiting the surface interactions between the drug and ion exchange groups that are necessary for adequate adsorption. Although reductions in heart and kidney tissue concentrations of DOX were observed during treatment with CF devices, liver tissue concentrations of DOX were slightly higher in the control animals, potentially due to recirculation of DOX. These results are comparable to those of previous reports evaluating extracorporeal hemofiltration of DOX in pigs (40). In that study, researchers concluded that the increased hepatic concentrations in control animals treated without hemofiltration may have been due to a net increase in the systemic distribution and subsequent recirculation of unmetabolized DOX to the liver. An additional potential limitation of our experimental design is that DOX might elute off our devices when they are retrieved, as potentiated by mechanical squeezing through the access sheath. Future experiments can address this issue; if this does occur, then devices could be retrieved inside an invertible bag, for example.

In conclusion, our study demonstrates that a reduction in systemic exposure and cardiac bioaccumulation of DOX during

local-regional chemotherapy to the liver can be achieved through selective adsorption by a minimally invasive image-guided CF device. We hypothesize that drug-specific adsorption was achieved by exploiting the affinity of the positively charged moiety of DOX toward the negatively charged sulfonic acid groups on SAC resins. High DOX extraction efficiencies are possible in situ using minimally invasive devices containing drug-specific binding materials.

**Acknowledgments:** This is a multidisciplinary effort sponsored by the National Cancer Institute (R01CA194533; principal investigator, Steven W. Hetts) involving investigators at multiple institutions. As such, all participants are part of the ChemoFilter Consortium and should be cited as collaborators. The Consortium's members include the following individuals and institutions: Steven W. Hetts (University of California, San Francisco [hereafter, UCSF]), Mark W. Wilson (UCSF), Anand Patel (UCSF), Shuvo Roy (UCSF), Henry VanBrocklin (UCSF), Terilyn Moore (UCSF), Carol Stillson (UCSF), Aaron Losey (UCSF), Caroline Jordan (UCSF), Colin Yee (UCSF), Bridget Kilbride (UCSF), Jon Chan (UCSF), Nitash Balsara (University of California, Berkeley), Hee Jeung Oh (University of California, Berkeley), Robert Grubbs (Caltech), Julia Greer (Caltech), Daryl Yee (Caltech), Sankarganesh Krishnamoorthy (Caltech), Carl Blumenfeld (Caltech), Michael Schulz (Virginia Tech), Vitaliy Rayz (Purdue), and Nazanin Maani (Purdue).

**Author contributions:** Guarantors of integrity of entire study, C.Y., D.M., T.M., S.W.H.; study concepts/study design or data acquisition or data analysis/interpretation, all authors; manuscript drafting or manuscript revision for important intellectual content, all authors; approval of final version of submitted manuscript, all authors; agrees to ensure any questions related to the work are appropriately resolved, all authors; literature research, C.Y., H.J.O., S.R., A.P., S.W.H.; experimental studies, C.Y., D.M., J.Y., A.L., C.J., T.M., C.S., H.J.O., B.K., M.W.W., S.W.H.; statistical analysis, C.Y., D.M., J.Y., C.J., H.J.O.; and manuscript editing, C.Y., D.M., J.Y., A.L., C.J., C.S., H.J.O., S.R., M.W.W., S.W.H.

**Disclosures of Conflicts of Interest:** C.Y. disclosed no relevant relationships. D.M. disclosed no relevant relationships. J.Y. disclosed no relevant relationships. A.L. disclosed no relevant relationships. C.J. disclosed no relevant relationships. T.M. disclosed no relevant relationships. C.S. disclosed no relevant relationships. H.J.O. Activities related to the present article: disclosed no relevant relationships. Activities not related to the present article: disclosed no relevant relationships. Other relationships: institution filed U.S. patent application no. PCT/US2019/29979. B.K. disclosed no relevant relationships. S.R. disclosed no relevant relationships. A.P. Activities related to the present article: disclosed no relevant relationships. Activities not related to the present article: is a consultant for Penumbra, Microvention, and Sirtex. Other relationships: has a patent pending for chemotherapy filtration. M.W.W. disclosed no relevant relationships. S.W.H. Activities related to the present article: disclosed no relevant relationships. Activities not related to the present article: is a consultant for Microvention and Terumo; institution previously received a licensing fee from Penumbra for the IP underlying the ChemoFilter device; a U.S. patent is pending, and an overseas patent has been granted in several countries. Other relationships: disclosed no relevant relationships.

## References

1. Siegel RL, Miller KD, Jemal A. Cancer statistics, 2018. *CA Cancer J Clin* 2018;68(1):7–30.
2. Memeo R, de Blasi V, Cherkaoui Z, et al. New Approaches in Locoregional Therapies for Hepatocellular Carcinoma. *J Gastrointest Cancer* 2016;47(3):239–246.
3. Llovet JM, Villanueva A, Lachenmayer A, Finn RS. Advances in targeted therapies for hepatocellular carcinoma in the genomic era. *Nat Rev Clin Oncol* 2015;12(7):408–424 [Published correction appears in *Nat Rev Clin Oncol* 2015;12(8):436.] <https://doi.org/10.1038/nrclinonc.2015.103>.
4. Lewis AL, Dreher MR. Locoregional drug delivery using image-guided intra-arterial drug eluting bead therapy. *J Control Release* 2012;161(2):338–350.
5. Gbolahan OB, Schacht MA, Beckley EW, LaRoche TP, O'Neil BH, Pyko M. Locoregional and systemic therapy for hepatocellular carcinoma. *J Gastrointest Oncol* 2017;8(2):215–228.
6. Cescon M, Cucchetti A, Ravaioli M, Pinna AD. Hepatocellular carcinoma locoregional therapies for patients in the waiting list. Impact on transplantability and recurrence rate. *J Hepatol* 2013;58(3):609–618.
7. Tam KY, Leung KCF, Wang YXJ. Chemoembolization agents for cancer treatment. *Eur J Pharm Sci* 2011;44(1-2):1–10.

8. Pascual S, Herrera I, Irurzun J. New advances in hepatocellular carcinoma. *World J Hepatol* 2016;8(9):421–438.
9. Budker VG, Monahan SD, Subbotin VM. Loco-regional cancer drug therapy: present approaches and rapidly reversible hydrophobization (RRH) of therapeutic agents as the future direction. *Drug Discov Today* 2014;19(12):1855–1870.
10. Deneve JL, Choi J, Gonzalez RJ, et al. Chemosaturation with percutaneous hepatic perfusion for unresectable isolated hepatic metastases from sarcoma. *Cardiovasc Intervent Radiol* 2012;35(6):1480–1487.
11. Rajeev R, Gamblin TC, Turaga KK. Hepatic Perfusion Therapy. *Surg Clin North Am* 2016;96(2):357–368.
12. Alexander HR Jr, Butler CC. Development of isolated hepatic perfusion via the operative and percutaneous techniques for patients with isolated and unresectable liver metastases. *Cancer J* 2010;16(2):132–141.
13. de Leede EM, Burgmans MC, Meijer TS, et al. Prospective Clinical and Pharmacological Evaluation of the Delcath System's Second-Generation (GEN2) Hemofiltration System in Patients Undergoing Percutaneous Hepatic Perfusion with Melphalan. *Cardiovasc Intervent Radiol* 2017;40(8):1196–1205 [Published correction appears in *Cardiovasc Intervent Radiol* 2017;40(12):1966.] <https://doi.org/10.1007/s00270-017-1630-4>.
14. Vahrmeijer AL, van Dierendonck JH, Keizer HJ, et al. Increased local cytostatic drug exposure by isolated hepatic perfusion: a phase I clinical and pharmacologic evaluation of treatment with high dose melphalan in patients with colorectal cancer confined to the liver. *Br J Cancer* 2000;82(9):1539–1546.
15. Glazer ES, Zager JS. Chemosaturation With Percutaneous Hepatic Perfusion in unresectable hepatic metastases. *Cancer Control* 2017;24(1):96–101.
16. Carvalho C, Santos RX, Cardoso S, et al. Doxorubicin: the good, the bad and the ugly effect. *Curr Med Chem* 2009;16(25):3267–3285.
17. Cummings J, Anderson L, Willmott N, Smyth JF. The molecular pharmacology of doxorubicin in vivo. *Eur J Cancer* 1991;27(5):532–535.
18. Chen XC, Oh HJ, Yu JF, et al. Block Copolymer Membranes for Efficient Capture of a Chemotherapy Drug. *ACS Macro Lett* 2016;5(8):936–941.
19. Patel AS, Saeed M, Yee EJ, et al. Development and Validation of Endovascular Chemotherapy Filter Device for Removing High-Dose Doxorubicin: Preclinical Study. *J Med Device* 2014;8(4):0410081–0410088.
20. Aboian MS, Yu JF, Gautam A, et al. In vitro clearance of doxorubicin with a DNA-based filtration device designed for intravascular use with intra-arterial chemotherapy. *Biomed Microdevices* 2016;18(6):98.
21. Dubbelboer IR, Lilienberg E, Hedeland M, Bondesson U, Piquette-Miller M, Sjögren E, et al. The effects of lipiodol and cyclosporin A on the hepatobiliary disposition of doxorubicin in pigs. *Mol Pharm*. 2014;11(4):1301–1313.
22. Lilienberg E, Dubbelboer IR, Sjögren E, Lennernäs H. Lipiodol does not affect the tissue distribution of intravenous doxorubicin infusion in pigs. *J Pharm Pharmacol* 2017;69(2):135–142.
23. Reddy LH, Meda N, Murthy RR. Rapid and sensitive HPLC method for the estimation of doxorubicin in dog blood—the silver nitrate artifact. *Acta Pharm* 2005;55(1):81–91.
24. Corrie PG. Cytotoxic chemotherapy: Clinical aspects. *Medicine (Baltimore)* 2011;39(12):717–722.
25. Poursaid A, Jensen MM, Huo E, Ghandehari H. Polymeric materials for embolic and chemoembolic applications. *J Control Release* 2016;240:414–433.
26. Agarwala SS, Eggermont AMM, O'Day S, Zager JS. Metastatic melanoma to the liver: a contemporary and comprehensive review of surgical, systemic, and regional therapeutic options. *Cancer* 2014;120(6):781–789.
27. Ahmad J, Akhter S, Greig NH, et al. Engineered Nanoparticles Against MDR in Cancer: The State of the Art and its Prospective. *Curr Pharm Des* 2016;22(28):4360–4373.
28. Wong HL, Bendayan R, Rauth AM, Xue HY, Babakhanian K, Wu XY. A mechanistic study of enhanced doxorubicin uptake and retention in multidrug resistant breast cancer cells using a polymer-lipid hybrid nanoparticle system. *J Pharmacol Exp Ther* 2006;317(3):1372–1381.
29. Brown KT, Do RK, Gonen M, et al. Randomized Trial of Hepatic Artery Embolization for Hepatocellular Carcinoma Using Doxorubicin-Eluting Microspheres Compared With Embolization With Microspheres Alone. *J Clin Oncol* 2016;34(17):2046–2053.
30. He C, Sun XP, Qiao H, et al. Downregulating hypoxia-inducible factor-2 $\alpha$  improves the efficacy of doxorubicin in the treatment of hepatocellular carcinoma. *Cancer Sci* 2012;103(3):528–534.
31. Jung EU, Yoon JH, Lee YJ, et al. Hypoxia and retinoic acid-inducible NDRG1 expression is responsible for doxorubicin and retinoic acid resistance in hepatocellular carcinoma cells. *Cancer Lett* 2010;298(1):9–15.
32. Reinhard K, Email A, Gailhofer S, Zavattieri G. Isolated Pelvic Perfusion with Chemofiltration for Pelvic Malignancies: Anal, Cervical, and Bladder Cancer. 2018;1–16.
33. van de Velde CJH, Kothuis BJJ, Barenbrug HWM, et al. A successful technique of in vivo isolated liver perfusion in pigs. *J Surg Res* 1986;41(6):593–599.
34. Alexander HRJ, Bartlett DL, Libutti SK. Current status of isolated hepatic perfusion with or without tumor necrosis factor for the treatment of unresectable cancers confined to liver. *Oncologist*. 2000;5(5):416–24.
35. Burgmans MC, de Leede EM, Martini CH, Kapiteijn E, Vahrmeijer AL, van Erkel AR. Percutaneous Isolated Hepatic Perfusion for the Treatment of Unresectable Liver Malignancies. *Cardiovasc Intervent Radiol* 2016;39(6):801–814.
36. Lienard D, Ewalenko P, Delmotte JJ, Renard N, Lejeune FJ. High-dose recombinant tumor necrosis factor alpha in combination with interferon gamma and melphalan in isolation perfusion of the limbs for melanoma and sarcoma. *J Clin Oncol* 1992;10(1):52–60.
37. Abbott AM, Doepker MP, Kim Y, et al. Hepatic Progression-free and Overall Survival After Regional Therapy to the Liver for Metastatic Melanoma. *Am J Clin Oncol* 2018;41(8):747–753.
38. Hughes MS, Zager J, Faries M, et al. Results of a Randomized Controlled Multicenter Phase III Trial of Percutaneous Hepatic Perfusion Compared with Best Available Care for Patients with Melanoma Liver Metastases. *Ann Surg Oncol* 2016;23(4):1309–1319.
39. Blumenfeld CM, Schulz MD, Aboian MS, et al. Drug capture materials based on genomic DNA-functionalized magnetic nanoparticles. *Nat Commun* 2018;9(1):2870.
40. August DA, Verma N, Vaerten MA, Shah R, Andrews JC, Brenner DE. Pharmacokinetic evaluation of percutaneous hepatic venous isolation for administration of regional chemotherapy. *Surg Oncol* 1995;4(4):205–216.